Available online at www.sciencedirect.com

SciVerse ScienceDirect

Ceramics International 39 (2013) 7751–7757

CERAMICS INTERNATIONAL

www.elsevier.com/locate/ceramint

Filamentous alumina–chitosan porous structures produced by gelcasting

Rafael Salomão[a,*], Jamile Brandi[b]

[a]Materials Engineering Department, São Carlos School of Engineering, University of São Paulo, Avenida Trabalhador São-carlense 400, 13566-590 São Carlos, SP, Brazil

[b]Federal University of the ABC Region (UFABC), Rua da Catequese 242, 09090-400 Santo André, SP, Brazil

Received 1 February 2013; received in revised form 3 March 2013; accepted 4 March 2013
Available online 22 March 2013

Abstract

Porous filamentous macroelements with tunable properties were developed using alumina–chitosan fibers produced by gelcasting extrusion. The initial suspension was prepared as a dilute aqueous acetic acid solution containing 13 vol% of alumina particles and 1.3 vol% of dissolved chitosan. After extrusion, coagulation in an NaOH bath and drying, 300 μm diameter continuous fibers (9 vol% of chitosan) were compacted and sintered at different temperatures (1100–1500 °C) to produce 40×40 mm^2 cylindrical macroelements. The effects of the thermal treatment temperature on the porosity, specific surface area, mechanical strength and microstructure of the macroelements were evaluated. It was verified that these properties can be controllably modified in a wide range, depending on the sintering conditions.

Keywords: Alumina; Chitosan; Gelcasting; Porous ceramics

1. Introduction

The lower toxicity and straightforward processing of alumina–chitosan suspensions have improved their usefulness in many gelcasting methods for ceramic processing [1–4]. Several studies have described the use of chitosan as a binding agent for monolithic parts [1,3,5], thick plates [6], films [7,8], fibers [9] and beads [10–12]. In aqueous acid suspensions (pH < 5), alumina shows a highly positive zeta potential [11,13,14] while chitosan remains dissolved as a positively charged polyelectrolyte [2,11,15]. Therefore, they can be mixed easily to produce stable suspensions, which are consolidated using crosslinking agents such as glutaraldehyde [6,16]. Because of the high molecular weight and intrinsically resistant chains of chitosan, strong bonds can be generated among alumina and other ceramic particles such as ZrO_2, SiO_2, Si_3N_4 and SiC [4,5,17,18].

Earlier studies describe a chitosan-based gelcasting method that produces spherical beads with adjustable characteristics [10–12]. In this method, a calcined alumina–chitosan suspension (2 wt% of chitosan in 0.1 M acetic acid solution, 13 vol% of solids, pH=4, Fig. 1a) is dripped (Fig. 1b) into a NaOH solution (pH = 14) and stirred. Due to the sudden variation in pH (Fig. 1c), the positively charged chitosan molecules adsorb onto the surface of negatively charged alumina particles and precipitate, preserving the spherical shape of the drops (Fig. 1d). By changing the volume of the drops, the diameter of the beads can be modified (from 0.3 up to 2 mm) and varying the drying and sintering conditions enables both porosity and specific surface area to be tuned (from 10 up to 80% and from 0.01 up to 3.5 m^2 g^{-1}, respectively).

Considering the many potential applications of this system, e.g., catalyst support [19], hot gas filtration [20], thermal insulation [20,21] and substrate for growing biological tissues [22], the production of a porous macrostructure which combines these microelements is an interesting point for investigation. Therefore, this paper describes an application for this gelcasting method to produce macroporous alumina–chitosan filamentous elements with tunable surface area and porosity. Instead of dripping, the alumina–chitosan suspension was extruded continuously in the NaOH coagulating bath to produce continuous fibers (Fig. 1e) [9]. The fiber geometry was chosen because, compared to the spherical shape of beads, filamentous elements show higher entanglement, which favors sintering and the development of mechanical strength.

*Corresponding author. Tel.: +55 16 33739576; fax: +55 16 3373 9590.
E-mail addresses: rsalomao@sc.usp.br (R. Salomão), jamilebrandi@gmail.com (J. Brandi).

0272-8842/$ - see front matter © 2013 Elsevier Ltd and Techna Group S.r.l. All rights reserved.
http://dx.doi.org/10.1016/j.ceramint.2013.03.032

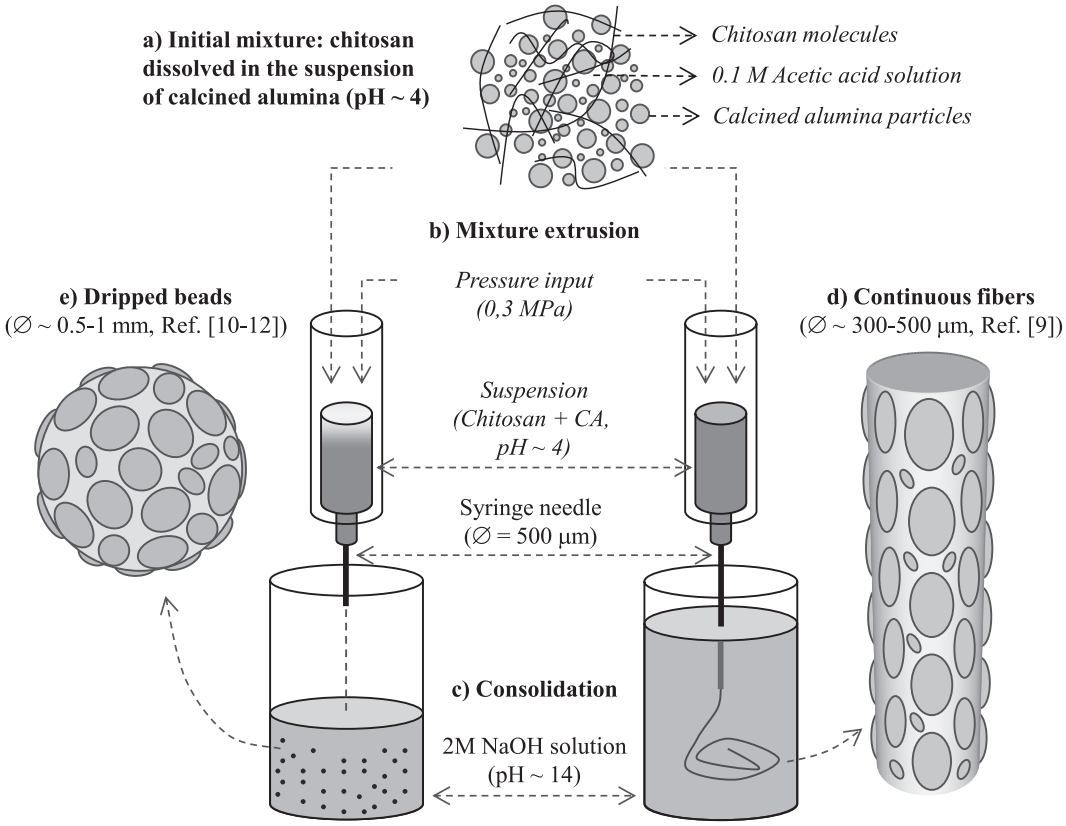

Fig. 1. Schematic representation of the consolidating method employed.

Table 1
Properties of the raw materials employed in the tests.

Calcined alumina (CA)[a]	
Chemical analysis (wt%; typical values)	α-Al_2O_3: 99.78; Na_2O: 0.08; Fe_2O_3: 0.02; SiO_2: 0.03; CaO: 0.02; MgO: 0.07
Specific surface area (BET method; m^2g^{-1})	7.2 ± 1.0
Particle size (μm; D_{50}/ D_{90})	0.61/ 0.95
Density (Helium picnometry; $g.cm^{-3}$)	3.98 ± 0.05 (before firing)
Isoelectric point (pH; dispersant-free)	8.5
Loss of ignition (%, 1000 °C)	0.81
Chitosan[b]	
Molecular weight (M_N, $g.mol^{-1}$)	54.350
Desacetilation degree (%)	96
Water solubility (pH range, at 25 °C)	≤6 (Reference 15)
Loss of ignition (%, 1000 °C)	97.8
Thermal decomposition (°C, T_{90}–T_{10})	219–505

[a]CT 3000 SG, Almatis, Germany.
[b]Polymar, Brazil.

Table 2
Compositions tested.

Alumina + Chitosan mixture			
Alumina suspension	Calcined alumina	40 vol%	50 vol%
	Acetic acid solution (0.1 M)	60 vol%	
Chitosan solution	Chitosan	2 wt%	50 vol%
	Acetic acid solution (0.1 M)	98 wt%	

The green fibers were vacuum compacted, bonded together using the same chitosan solution, and sintered, resulting in macroporous elements, which were then analyzed in terms of their porosity, surface area and mechanical strength after firing at different temperatures.

2. Materials and methods

A chitosan solution (2 wt% of chitosan in 0.1 M acetic acid solution, pH=4) was stirred at 40 °C for 24 h until the polymer was completely dissolved (Table 1). Calcined alumina (CA, CT3000SG, Almatis, Germany) was dispersed in a 0.1 M acetic acid solution (40 vol% of solids, pH=4.0) using a paddle mixer (RW20, IKA, Germany). After 5 min of stirring at 1000 rpm, the suspensions were deaerated for 1 h. Equal volumes of the chitosan solution and the CA suspension were mixed at 100 rpm for 5 min (Fig. 1a) to generate a system containing 13 vol% of solids and 1.3 vol% (1 wt%) of dissolved organics (after drying, the chitosan content in the system increased up to 2.6 wt%/9 vol%) (Table 2).

The zeta potential of the CA particles (plain and with chitosan) was measured in different pH ranges, using 2 vol%

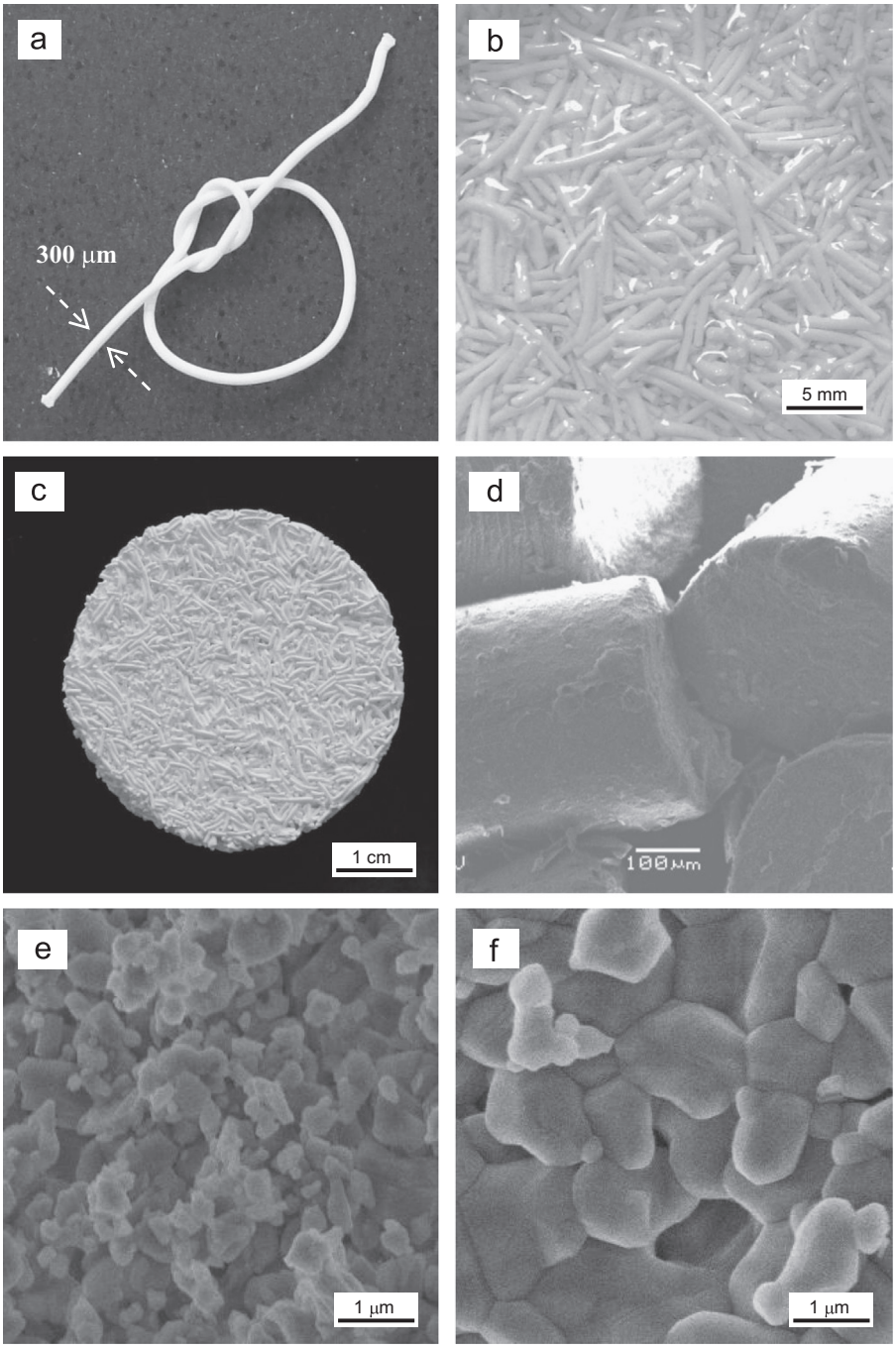

Fig. 2. (a) Aspect of the fibers attained just after coagulation and washing; (b) fibers during the compacting using chitosan solution as a binder; (c) and (d) macroelements after sintering at 1500 °C; (e) and (f) fracture surface of the fibers before and after sintering at 1500 °C, respectively.

of diluted suspensions (DT-1202, Dispersion Technology Inc., USA). The role of pH in the solubility of chitosan was evaluated based on turbidity tests, using a UV–vis spectrophotometer (Carry 50, Varian, USA), following a methodology described elsewhere [11,15].

The CA–chitosan suspensions (Fig. 1a) were then poured into a syringe connected to an air compressor (constant pressure of 30 kN m^{-2}, Fig. 1b) and the tip of the needle (500 μm × 10 mm) was inserted under the surface of a stirred 10 °C 2 M NaOH solution. In contact with this cold, anionic and high pH coagulation bath, the chitosan molecules rapidly precipitated, constraining the mobility of the particles (Fig. 1c). Because the extrusions were carried out continually, 300–500 μm diameter continuous fibers were obtained (Fig. 1e) [9,11] (by dripping the suspension, beads can be produced [11], Fig. 1d). After soaking in the solution for 1 h to ensure complete coagulation, the fibers were washed until their pH became neutral and then dried for 24 h at 80 °C. The as-received raw materials and dried green fibers were subjected to thermogravimetry tests (TGA-Q50, TA Instruments, 10 °C min^{-1}, 25–800 °C, and synthetic air atmosphere).

The fibers resulting from the above described coagulation and washing procedure were flexible (Fig. 2a). However, after drying at 80 °C, they became brittle because, despite its good mechanical strength, chitosan is a fragile polymer whose content in the composition was very low. Therefore, to produce the macroelements, the dried fibers were placed in a rotary plastic cylinder (diameter = 10 cm, height = 30 cm, 60 rpm, without milling elements), and left there for 60 min. This procedure reduced their lengths from continuous to a homogeneous condition of approximately 5 mm (Fig. 2(a) and (b)). The fibers were then compacted under vibration in cylindrical molds (40 mm × 40 mm), into which a solution of 2 wt% of chitosan in 0.1 M acetic acid was poured to completely fill the inter-fiber spaces (Fig. 2b). The excess chitosan was removed by vacuum filtering and, after drying for 24 h at 80 °C, the dried green macroelements were demolded and sintered (1100–1500 °C, 1 °C min^{-1} up to 600 °C, 5 °C min^{-1} up to maximum temperature for 5 h, followed by cooling at a rate of 5 °C min^{-1}) (Fig. 2c and d).

The specific surface area (SSA), mechanical strength, porosity and solid density (ρ) of the sintered macroelements were measured. For the SSA (BET method, Nova 1200e, Quantachrome Instruments, USA, ASTM C1069–09) and ρ (Helium pycnometry, Ultrapyc 1200e, Quantachrome Instruments, USA) measurements, 8 × 8 mm^2 cylindrical samples were extracted from the main piece using a cup bit drill. The mechanical strength was measured under diametrical compression, according to the ASTM C496-90 standard, in an MTS 810 TestStar II material testing system at a loading rate of 2 N s^{-1}. Seven samples were tested for each condition.

The porosity of this type of structure can typically be divided into two categories [20,21]: (1) discontinuous intra-fiber porosity (IntraP) inside the microstructure of the fibers, and (2) continuous inter-fiber macroporosity (InterP) between the fibers. Although common porosity measuring techniques such as the Archimedes method and Hg intrusion are easily used to identify the first class of pores, they are not suitable for the second category. The reason for this is that when pores are larger than 500 μm, there is no clear demarcation between pores and external surfaces [20]. Therefore, two different approaches were employed to characterize the elements. The IntraP was determined using the Archimedes method and ethanol as immersion fluid (in each measurement, excess ethanol between the fibers was removed carefully before each mass recording). The total porosity of the elements (TP) and the InterP were measured by the geometric method, which calculates the total porosity of the system (TP) based on the density of the fibers attained at each sintering temperature, using Helium pycnometry (ρ_S) and external volume (V_T) of the samples according to Eqs. 1 and 2

$$TP\ (\%) = 100\% \times (V_T - (M_S/\rho_S))/V_T \quad (1)$$

$$InterP\ (\%) = TP - IntraP \quad (2)$$

where M_S is the mass of the sample. For each condition, 5 samples were tested.

The volumetric shrinkage (VS) was calculated by measuring the external volume of the samples before ($V_{Initial}$) and after (V_{Final}) thermal treatment and using the following equation:

$$VS(\%) = 100\% \times (V_{Initial} - V_{Final})/V_{Initial} \quad (3)$$

The microstructure of the elements was examined by scanning electron microscopy (SEM, Philips XL30 FEG).

3. Results and discussion

3.1. Preparation and characterization of the CA-chitosan fibers

In acid pH (below 6, Fig. 3), chitosan molecules behave as a positively charged polyelectrolyte, generating a stable solution (high transmittance), while the CA particles show highly positive charged surfaces [11,13–15]. This condition allows for the preparation of a highly solid load of well dispersed chitosan containing CA suspensions (Fig. 1a) and its extrusion through a syringe with a fine gauge needle (Fig. 1b).

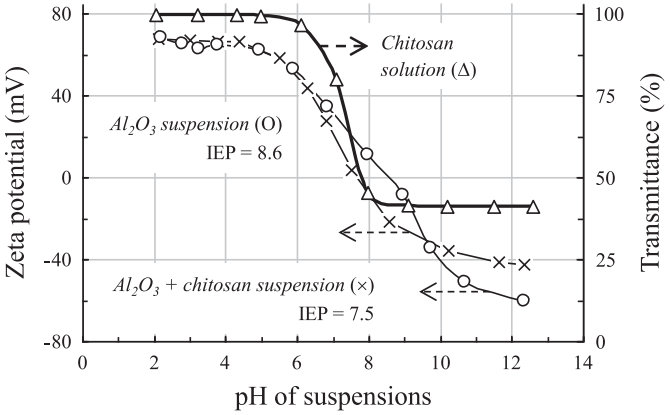

Fig. 3. Zeta potential versus pH behavior for the plain alumina and alumina-chitosan suspensions. The effect of pH on chitosan solubility (at 25 °C) is shown using the UV–vis transmittance.

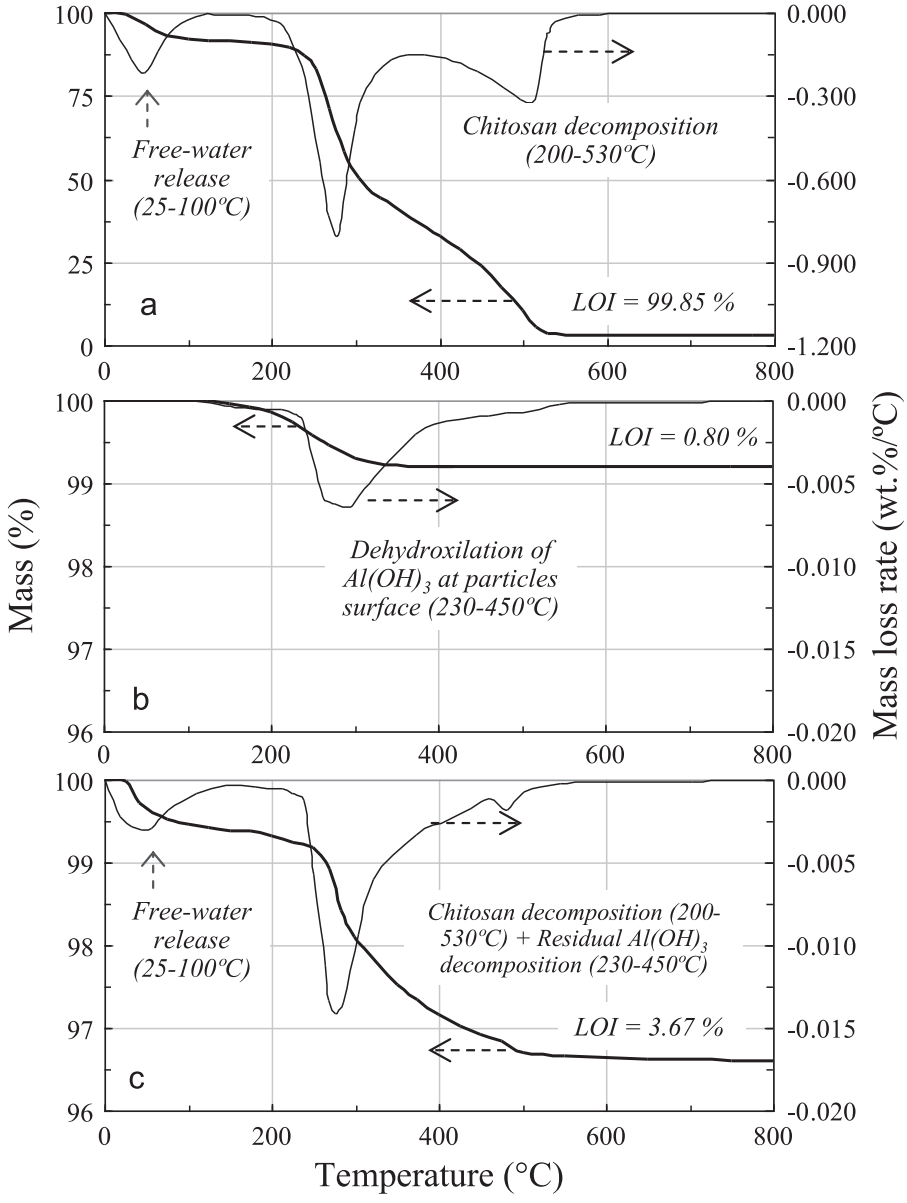

Fig. 4. Thermogravimetry for as-received (a) chitosan, (b) calcined alumina and (c) dried green fibers.

Pouring the suspension into the NaOH coagulation bath caused the pH to increase abruptly to above 6, producing a combination of two effects that contributed to consolidate the system. (1) The addition of chitosan shifted the CA isoelectric point (IEP) to lower pH values (from 8.5 to 7.5) [11,14] and reduced the zeta potential levels attained at pH values above 9, due to a mutual partial neutralization of charges. This effect indicates that the negatively charged CA particles behaved as adsorption sites for the positively charged chitosan molecules [2]. (2) As a result of the contact with the cold alkaline anionic coagulation bath, chitosan precipitates as gel due to the deprotonation of the $(R\text{-}NH_3)^+$ groups [11,15], further constraining particle mobility. Because this consolidation mechanism occurs almost instantaneously, the initial shape the suspension assumes upon its first contact with the coagulation bath is preserved. Therefore, beads are produced by dripping the suspension [10–12]. On the other hand, by inserting the tip of the needle into the solution, the extrusion of the suspension produces a continuous flexible fiber-shaped circular profile (Fig. 2).

The raw materials employed were characterized by thermogravimetry in earlier studies [11,23]. Chitosan exhibits a mass loss behavior consisting of three main sequential events: the release of free water up to 150 °C and two sequential intense mass loss stages between 170–380 °C and 380–560 °C, which are related, respectively, to the decomposition of the main polymeric chain and the final oxidation of the carbonaceous residues formed (Fig. 4a) [11,23]. Calcined alumina undergoes a slight mass loss (0.8 wt%) due to surface dehydroxylation (Fig. 4b). Most of the mass loss of the dried green fibers can be attributed to drying up of the residual free water and decomposition of chitosan (Fig. 4c). The low value of total mass loss at 800 °C (3.7 wt%) is an important technological advantage of this gelcasting method. Because it requires a very small amount of chitosan for

consolidation, the first heating before sintering can be carried out without worrying about the generation of volatiles and cracking during polymer burnout.

3.2. Preparation and characterization of the filamentous elements

Fig. 2c and d illustrates the filamentous elements after sintering, while Fig. 2e and f shows the fracture surface of green fibers and fibers sintered at 1500 °C. Note the homogeneous distribution of the fibers and the welded points between adjacent fibers, which give the structure its mechanical strength.

The results of porosity, volumetric shrinkage, mechanical strength and specific surface area (Fig. 5) indicate that the microstructure of the samples underwent several changes after sintering. The porosity results measured by the Archimedes method (IntraP, Fig. 5a) correspond to the smallest pores located inside the fiber microstructure (average diameter around 1 μm, Fig. 2e and f), which were formed mainly due to packing flaws among the particles filled with water, chitosan or air bubbles at the moment of consolidation. These results indicate that because no external compaction pressure such as isostatic pressing was applied to the samples before sintering, the highly porous structure of the as-spun fibers was partially preserved after drying and sintering. Starting from a value of 25.4% for the green dried samples, the IntraP level initially increased to 39.6% in response to firing at 1100 °C as a result of chitosan decomposition and the removal of residual water. However, heating above this temperature increased the driving force of sintering and reduced the IntraP and specific surface area of the samples.

The InterP results (Fig. 5a) correspond to voids among the fibers that are too large to be detectable by the Archimedes method. As the fibers became denser in response to decreasing IntraP, a slight enhancement of the contribution of the InterP values to the TP results was observed. This behavior suggests that the spaces between fibers increased as the latter became denser and thinner. It is also worth noting that, despite the decrease in TP, the volumetric shrinkage levels attained were quite low even at the highest sintering temperatures.

Compared with the green dried samples, the strength of samples fired at 1100 °C was significantly lower (Fig. 5b). This decline in strength was attributed to the burnout of chitosan, which kept the alumina particles bound together, and with the consequent enhancement in porosity combined with a low sintering level. As the thermal treatment temperatures rose, the strength increased to levels similar to those of other porous structures reported in the literature (with similar degrees of

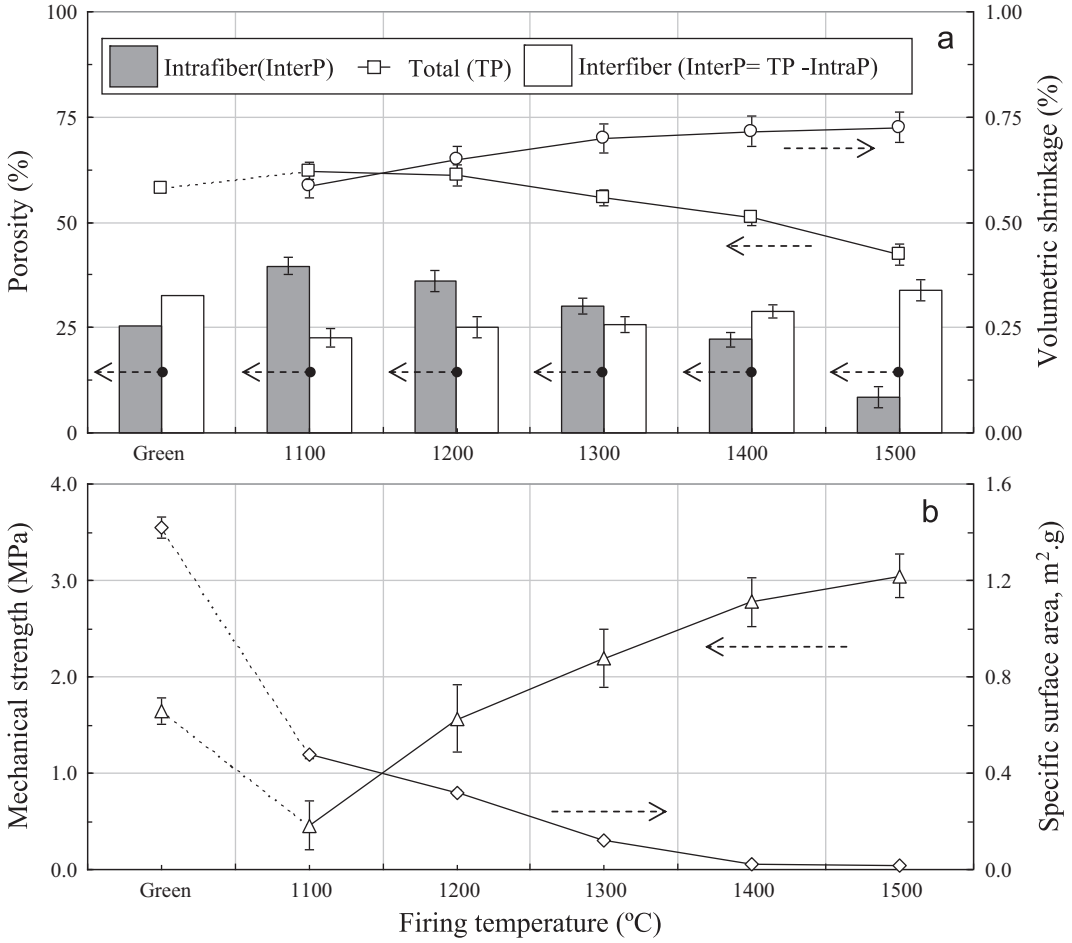

Fig. 5. (a) Porosity and volumetric shrinkage and (b) mechanical strength and specific surface area for the green and sintered filamentous macroelements.

relative density [21]), rendering the samples suitable for cup-drilling and grinding. In this case, the augmented strength is caused by two effects: (1) sintering of the alumina particles and reduction of the porosity inside each fiber, and (2) bond welding at the points where fibers touch each other.

4. Final remarks

A novel family of porous filamentous macroelements with tunable properties was developed using alumina–chitosan fibers produced by gelcasting extrusion. These macroelements, which can be used in different applications such as high temperature filtration, catalysis, thermal insulation and support for biological tissue growth, were produced in a two-step process. First, alumina particles were shaped into 300 μm diameter fibers using chitosan as a bonding agent to ensure suitable green strength for handling. Chitosan was then used again to consolidate the vacuum compacted fibers prior to the thermal treatment. Due to the low content of chitosan inside the fibers (lower than 3 wt% in the dried fibers), its thermal decomposition did not significantly affect the heating schedule. By balancing the sintering temperature (from 1100 °C to 1500 °C), the porosity inside (intra-fiber porosity) and among (inter-fiber porosity) the fibers, mechanical strength and specific surface area can be controlled. Studies are being conducted by the author's research group to produce macroelements using other raw materials, such as aluminum hydroxide and silica.

Acknowledgments

The authors would like to acknowledge the Brazilian Research Foundations FAPESP and CNPq for supporting this research and Almatis (Brazil and Germany) for kindly supplying the samples of raw materials.

References

[1] S.B. Johnson, D.E. Dunstan, G.V. Franks, Rheology of cross-linked chitosan-alumina suspensions used for a new gelcasting process, Journal of the American Ceramic Society 85 (7) (2002) 1699–1705.
[2] C. Pagnoux, M. Mougenot, P.G. Perez, T. Chartier, J.F. Baumard, Coagulation of mixed organic systems and alumina particles for paste production, Journal of the European Ceramic Society 26 (2006) 3091–3098.
[3] E. Chevalier, D. Chulia, C. Pouget, M. Viana, Fabrication of porous substrates: a review of processes using pore forming agents in the biomaterial field, Journal of Pharmaceutical Science 97 (3) (2008) 1135–1154.
[4] J. Yang, J. Yu, Y. Huang, Recent development in gelcasting ceramics, Journal of the European Ceramic Society 31 (2011) 2569–2591.
[5] M. Bengisu, E. Yilmaz, Gelcasting of alumina and zirconia using chitosan gels, Ceramics International 28 (2002) 431–438.
[6] L.J. Bonderer, A.R. Studart, J. Woltersdorf, E. Pippel, L.J. Gauckler, Strong and ductile platelet-reinforced polymer films inspired by nature: microstructure and mechanical properties, Journal of Materials Research 24 (9) (2009) 2741–2754.
[7] F. Sun, B.K. Lim, S.C. Ryu, D. Lee, J. Lee, Preparation of multi-layered film of hydroxyapatite and chitosan, Materials Science and Engineering C 30 (2010) 789–794.
[8] X. Wang, B. Zhang, X. Liu, J.Y.S. Lin, Synthesis of *b*-oriented TS-1 films on chitosan-modified alpha-alumina substrates, Advanced Materials 18 (2006) 3261–3265.
[9] S. Mohanty, A.P. Rameshbabu, S. Dhara, Alpha-alumina fiber with platelet morphology through wet spinning, Journal of the American Ceramic Society 95 (4) (2012) 1234–1240.
[10] H.V. Fajardo, A.O. Martins, R.M. De Almeira, L.K. Noda, L.F.D. Probst, N.L.V. Carreño, A. Valentini, Synthesis of mesoporous Al_2O_3 macroespheres using the biopolymer chitosan as a template: A novel active catalyst system for CO_2 reforming of methane, Materials Letters 59 (2005) 3963–3967.
[11] J. Brandi, J.C. Ximenes, M. Ferreira, R. Salomão, Gelcasting alumina-chitosan beads, Ceramics International 37 (4) (2011) 1231–1235.
[12] G.D.B. Nuernberg, E.L. Foletto, L.F.D. Probst, C.E.M. Campos, N.L.V. Carreño, M.A. Moreira, A novel synthetic route for magnesium aluminate ($MgAl_2O_4$) particles using metal-chitosan complexation method, Chemical Engineering Journal 193–194 (2012) 211–214.
[13] J.A. Lewis, Colloidal processing of ceramics, Journal of the American Ceramic Society 83 (10) (2000) 2341–2359.
[14] G.V. Frankes, Y. Gan, Charging behavior at the alumina-water interface and implications for ceramic processing, Journal of the American Ceramic Society 90 (11) (2007) 3373–3388.
[15] C. Qin, H. Li, Q. Xiao, Y. Liu, J. Zhu, Y. Du, Water solubility of chitosan and its antimicrobial activity, Carbohydrate Polymers 63 (2006) 367–374.
[16] S. Lin-Gibson, H.J. Walls, S.B. Kennedy, E.R. Welsh, Reaction kinetics and gel properties of blocked diisocyinate crosslinked chitosan hydrogels, Carbohydrate Polymers 54 (2003) 193–199.
[17] L Saravanan, S. Subramanian, A.B.V. Kumar, R.N. Tharanathan, Surface chemical studies on SiC suspensions in the presence of chitosan, Ceramics International 32 (2006) 637–646.
[18] S. Chen, A. Osaka, K. Tsuru, S. Hayakawa, Preparation and biomineralization of silica-based organic–inorganic hybrid hollow nanoparticles for bone tissue generation, in: R. Narayan, P. Colombo, T. Ohji, A. Wereszczak (Eds.), Proceeding of the 32nd International Conference on Advanced Ceramics and Composites, Advances in Bioceramics and Porous Ceramics, Daytona Beach, Florida, USA, 2008.
[19] E. Guibal, Heterogeneous catalysis on chitosan-based materials: a review, Progress in Polymer Science 30 (2005) 71–109.
[20] F. Schüth, K. Sing, Definitions, terminology and classification of pore structures, in: F. Schüth, K. Sing, J. Weitkamp (Eds.), Handbook of Porous Solids, Vol. I, Wiley-VCH, Weinheim, Germany, 2002.
[21] A.R. Studart, U.T. Gonzenbach, E. Tervoot, L.J. Gauckler, Processing routes to macroporous ceramics: a review, Journal of the American Ceramic Society 89 (6) (2006) 1771–1789.
[22] M.R. Gandhi, N. Viswanathan, S. Meenakshi, Preparation and application of alumina-chitosan biocomposite, International Journal of Biological Macromolecules 47 (2010) 146–154.
[23] F.A. López, A.L.R. Mercê, F.J. Alguacil, A. López-Delgado, A kinetic study on the thermal behavior of chitosan, Journal of Thermal Analysis and Calorimetry 91 (2008) 633–639.